Applied Innovative Research
Vol. 2, June 2020, pp.

Photoluminescence study of $Sr_3Y_{1-X}(BO_3)_3:_xTb^{3+}$ green emitting phosphor

S P Hargunani[a*], R S Palaspagar[b], R P Sonekar[a] & S K Omanwar[c]

[a]Department of Physics, G S College khamgaon, Dist: Buldana 444 303, India
[b]Department of Physics, Shivramji Moghe Mahavidyalaya, Kelapur (Pkd) Dist Yavatmal 445 302, India
[c]Physics Department, S G B A U Amravati 444 602, India

Received 26 June 2019; Accepted 20 March 2020

Terbium doped strontium yttrium borate phosphor is prepared by solution combustion method. Structural characterization of $Sr_3Y(BO_3)_3:Tb^{3+}$ (SYB:Tb) has been carried out with X-ray powder diffraction (XRD) analysis. Particle size of 0.5–2 µm and perfect element composition were seen in SEM-EDS. Using FTIR at room temperature the presence of $[BO_3]^-$ group; complete combustion of nitrates, organic material, absence of O-H bond were firmed up. Photoluminescence properties of the phosphor have been investigated by measuring the excitation and emission spectra. Several luminescence bands of Tb^{3+} ions are observed under 233 nm excitation wavelengths in 350–700 nm spectral region. The emission spectra were composed of three bands, in which the dominated emission of green luminescence SYB:Tb attributed to the transition $^5D_4 \rightarrow {}^7F_5$ is centered at 543 nm. The dependence of the emission intensity on the Tb^{3+} concentration for the $Sr_3Y_{1-X}(BO_3)_3:_xTb^{3+}$ ($0.01 \leq x \leq 0.05$) was studied and observed that the optimum concentration of Tb^{3+} in phosphor was 3 mol% for the highest emission intensity at 543 nm. The CIE coordinates (X=0.251363409, Y=0.736605581) fall at the border of green region in the CIE 1931 chromaticity.

Keywords: Photoluminescence, Green emission, Borate phosphors, Solution combustion method

Introduction

The increasing variety of borate materials were widely investigated due to their wide applications in nonlinear optics (NLO), plasma display panel (PDP) display and white light-emitting-diodes (LEDs)[i-ii-iii-iv]. In the recent decades, phosphors have undergone a fast growth because of their unique luminescence properties (such as long lifetime, high efficiency, adjustable spectrum, et cetera) and indispensable roles in a wide range of application, especially in the field of white light-emitting diodes (w-LEDs)[i-ii-iii] and field emission displays (FEDs). Recently, White light-emitting diodes (LEDs) have been widely applied as backlight units in modern LCD technologies to achieve larger color gamut, higher brightness, and lower power consumption[i-ii-iii]. In fact, the local structure and crystal environment have a great influence on the optical properties of activator ions, so finding an excellent host material is very needful. Single-phase borates had been researched widely because their crystal structures facilitate rare earth ions doped and represent not only the preferable thermal and chemical stability but also the various structures have examined their efficiency as luminescent materials[i]. Although the coordination modes of single-phase borates are different in these synthetic compounds, the host lattice of single-phase borates is considered suitable and easy to contain a variety of rare earth ions because of their similar ionic radii. Researchers from all over world are working in the direction of developing new phosphor materials in different wavelength range i.e. blue (435–500 nm), green (520–565 nm), yellow (565–590), and red (625–740 nm). Green phosphor used in NUV-WLED, blue-WLED convert radiation in the ranges 320–410 or 450–480 nm to light centered in the green region (520–565 nm). [i]Synthesis of strontium rare-earth borates described by the formula $Sr_3Ln(BO_3)_3$ (Ln = Y,Pr–Lu)was reported by Khamaganova *et al.* [i] $Sr_3Y(BO_3)_3$ crystal is a promising laser host material. Chemically and thermally stable borate phosphors $(Sr,Ba)_3(Y,La)(BO_3)_3$ are efficiently excited by UV light with tunable emission wavelength ranging across the visible spectrum from blue to red[i].

Borate compounds of the family $A_3RE(BO_3)_3$ (A = Ba, Sr; RE =Y, La) have been studied primarily for solid-state laser host materials with other activator ions including Er^{3+}, Yb^{3+},Er^{3+}/Yb^{3+} pairs, Nd^{3+}, Pr^{3+} and Tm^{3+}. They have also been studied under vacuum-ultraviolet excitation for fluorescent lamps

*Corresponding author: (E-mail: sphargunani.sh@gmail.com)

and plasma displays using Tb^{3+} as an activator ion with Ce^{3+} substituted $Sr_3Y(BO_3)_3$ reported as a scintillation material[xi]. Trivalent terbium Tb^{3+} ion is used as a green emitting center in a variety of commercial phosphors. The electronic configuration of Tb^{3+} ion is $^4f_8$. In case of Tb^{3+} ion, the absorption is usually due to allowed f-d transition. From excited state of $^4f_7$-$^5d_1$ configuration, the electron loses energy to lattice and comes to ^5D_j. $^5D_3 \rightarrow {}^7F_j$ emission is in UV and blue region while $^5D_4 \rightarrow {}^7F_j$ emission is predominantly green. At lower concentrations, blue emission is observed, but at higher concentration, there is an energy transfer between Tb^{3+} ions, e.g. the cross relaxation- Tb^{3+} ($^5D_3$) + Tb^{3+} (^7F_j) → Tb^{3+} ($^5D_4$) + Tb^{3+} ($^7F_0$), due to which the blue emission gets quenched increasing the green emission at the same time. In the present work we synthesized the $Sr_3Y(BO_3)_3$ as polycrystalline borate phosphor host for Tb^{3+} ion and studied its photoluminescence characteristics.

Experimental Details

Given Inorganic borate phosphors were prepared by the modified solution combustion synthesis technique[i]. In this technique urea is used as fuel and nitrates are oxidizer. Stoichiometric amounts of high purity starting materials, $SrNO_3$ (A.R.), $Tb_2(SO_4)_3.8H_2O$ (high purity 99.9%), H_3BO_3 (A.R.), $CO(NH_2)_2$ (A.R.), $Y(NO_3)_3$ (A.R.) are used for phosphor preparation. The starting materials with little amount of double distilled water were mixed thoroughly in agate mortar to obtain a homogeneous solution. Excess water was removed by heating the samples at temperature 80 °C for about 2 h on magnetic stirrer- heater and the solution was then transferred directly to a pre-heated Muffle furnace, maintained at temperature 850 °C, for combustion. As shown in Fig.1. Following the combustion, the resulting foamy samples was crushed to obtain fine particles and then annealed for 3 h at temperature

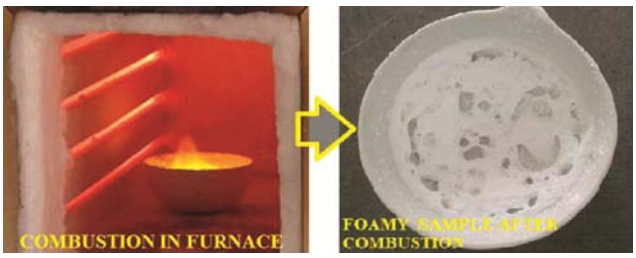

Fig. 1 — Solution combustion in furnace and foamy sample after combustion

1050 °C. The phase identification was performed by X-ray powder diffraction analysis using a Rigaku Miniflex II X-ray Diffractometer with Cu Ka radiation (k = 1.54060 Å). The excitation and emission spectra were recorded by use of a Hitachi F-7000 Fluorescence Spectrophotometer. Scanning electron microscopy (FEI Quanta200F) was used for the observation of particle morphology. All measurements were carried out at the same conditions.

Results and Discussion

The prepared materials were characterized by powder XRD, SEM, PL and FT-IR techniques. Powder X-ray diffraction measurements were taken on a Rigaku Miniflex II X-ray Diffractometer and compared with ICSD files. Surface morphology and elemental analysis of the calcined powder sample was observed by scanning electron microscopy [SEM: Model JSM6100 (Jeol)]. PL and PLE measurements at room temperature were performed on a Hitachi F-7000 spectroflurometer with spectral resolution of 2.5 nm. FTIR of sample was done on F.T. Infra-Red Spectrophotometer Model RZX (Perkin Elmer).

XRD

SYB:Tb with different Tb^{3+} contents have a similar XRD pattern. Fig. 2 shows the XRD pattern of SYB:Tb (3 mol%) using the Cu-Kα wavelength (k = 1.54060 Å) in the range of 2h from 5 ° to 80°. The peaks of the XRD pattern well match with those of SYB crystal. Because of the Y^{3+} (1.02 Å) contraction, rare earth ions have similar radius, coordination environment and physical–chemical properties. When Y^{3+} in SYB lattice is replaced by Tb^{3+}, the crystal structure does not change dramatically, which is similar to that of SYB.

FTIR

The FT-IR spectra of $Sr_3Y_{1-0.03}(BO_3)_3{:}_{0.03}Tb^{3+}$ recorded at room temperature is shown in Fig. 3. The strong bands observed above 1100 cm^{-1} should be assigned to the B-O stretching mode of the triangular $[BO_3]^-$ groups, while the bands with maxima at about 700-800 cm^{-1} should be attributed to the B-O out of plane bending, which confirms the existence of the $[BO_3]^-$ groups[10]. The absence of peaks in 1500- 2000 cm^{-1} indicates the complete combustion of nitrate and organic matter. The peak at 3300-3500 cm^{-1} corresponds the stretching mode of O-H are also absent.

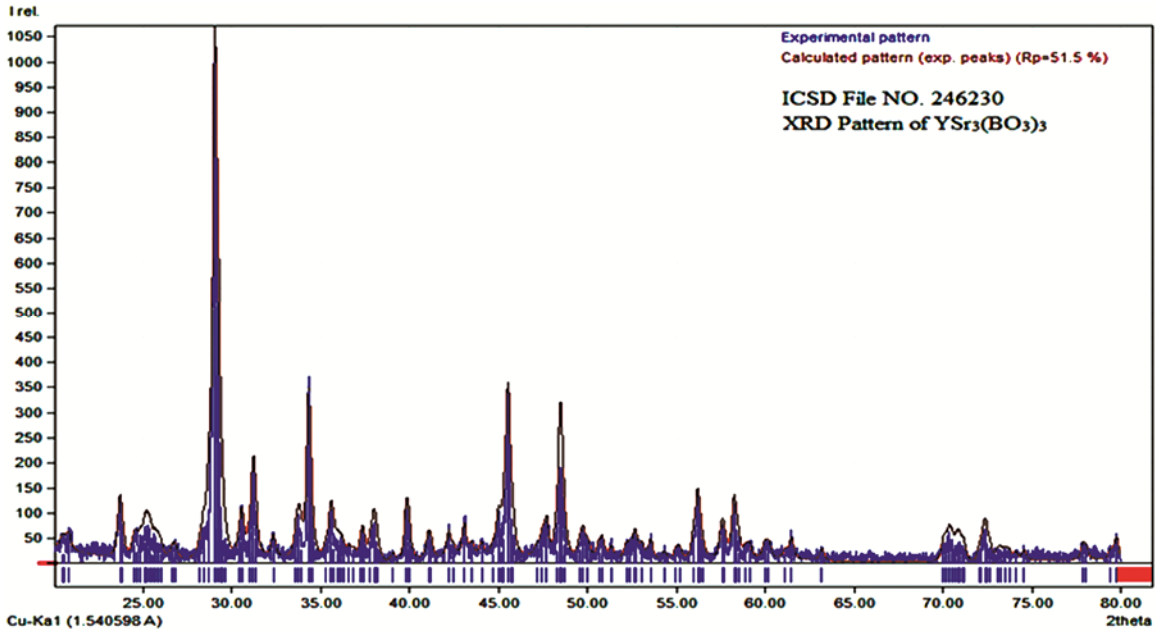

Fig. 2 — XRD pattern of $Sr_3Y_{1-0.03}(BO_3)_3{:}_{0.03}Tb^{3+}$

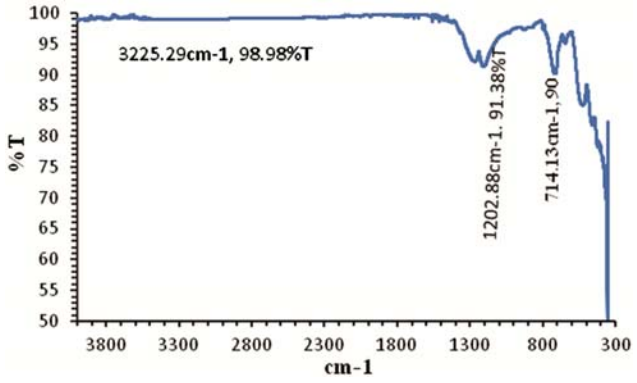

Fig. 3 — FTIR spectra of $Sr_3Y_{1-0.03}(BO_3)_3{:}_{0.03}Tb^{3+}$ recorded at room temperature

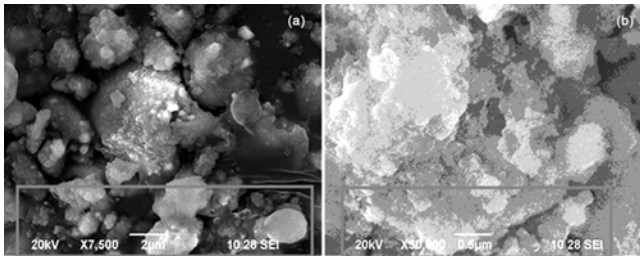

Fig. 4 — SEM images of $Sr_3Y_{1-0.03}(BO_3)_3{:}_{0.03}Tb^{3+}$

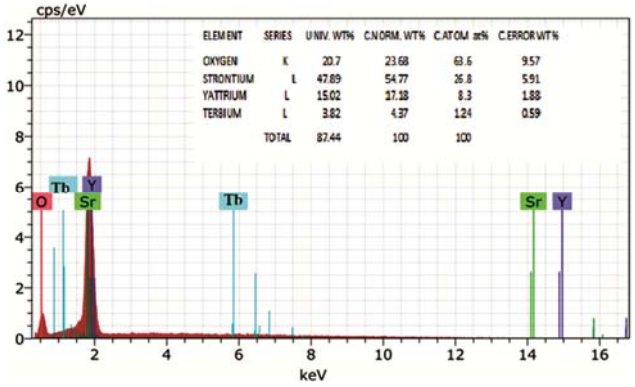

Fig. 5 — Element composition map of $Sr_3Y_{1-0.03}(BO_3)_3{:}_{0.03}Tb^{3+}$ phosphor

SEM and eds

The morphology of sample was studied using Scanning electron microscopy. The SEM images of $Sr_3Y_{1-0.03}(BO_3)_3{:}_{0.03}Tb^{3+}$ phosphors are shown in Fig. 4. It was observed that the microstructure of the phosphor consisted of irregular grains with agglomerate phenomena. The average size of synthesized phosphor particles is about 0.5–2 μm. The results show that phosphors have a good crystallinity and a relatively low sinter temperature. Average crystalline size by Scherrer formula is in 42.2 nm which is different than as seen in surface morphology. It is because SEM shows the image of polycrystalline particles and XRD measurements reflects the crystalline domain size. EDS or element composition map of material is given in Fig. 5. EDS cannot detect the lightest element boron B of the prepared phosphor because of instrument and operating conditions like the detector window is equipped with Be. The percentage composition of all elements matches with the EDS mapping of phosphor.

PL and PLE

The PL and PLE of $Sr_3Y_{1-0.03}(BO_3)_3{:}_{0.03}Tb^{3+}$ phosphor is shown in Fig. 6. It is recorded on F-7000 FL spectrophotometer with scan speed 240 nm/min, excitation-emission slit width 1nm. The excitation spectrum of $Sr_3Y_{1-0.03}(BO_3)_3{:}_{0.03}Tb^{3+}$ consists of a single broadband absorption ranging from 200 to 350 nm with the single peak at 233 nm which may be due to the electronic transitions from the ground state $^7F_6$ to the excited state $^5D_4$ of Tb^{3+} ions. At 233 nm excitation, SYB:Tb exhibit a broad emission band in the range 350−700 nm, which originates from the excited $^5D_4$ to ^7F_i (i=6, 4, 3, 2,1, and 0). 489 nm peak is due to $^5D_4$ to $^7F_6$; Strongest peak 543 nm is due to $^5D_4$ to $^7F_5$; 587 nm peak is due to $^5D_4$ to $^7F_4$ and 625 nm is due to $^5D_4$ to $^7F_3$ electronic transitions of Tb^{3+} ions. Intensity at 489 nm is about half the intensity at 543 nm. Intensity of emission lines at 587 nm and 625 nm is very low. $^5D_4$ to $^7F_5$ green emission line is the strongest because this transition has the largest probability for both electric-dipole and magnetic-dipole induced transitions[ii].

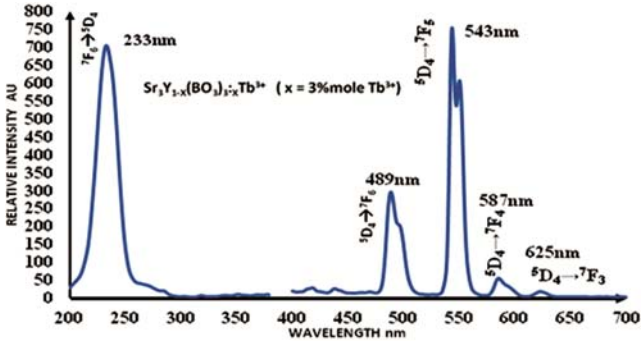

Fig. 6 — PL and PLE of $Sr_3Y_{1-0.03}(BO_3)_3{:}_{0.03}Tb^{3+}$

We studied the PL properties for $^5D_4$ to $^7F_5$ transition with different doping concentrations of Tb^{3+} activator ion. The emission spectra of SYB:Tb excited by 233 nm at room temperature and electronic transitions is similar to the emissions is shown in Fig. 7 (a & b). The shape of PL band is same and intensity of emission increases from 1 mole% up to 3 mole % of Tb^{3+} and then decreases. The luminescence of Tb^{3+} depends upon the site occupied and crystal structure of host lattice. The variation of intensity for $^5D_4$ to $^7F_5$ transition with Tb^{3+} concentration is shown in Fig. 8. Intensity of 543 nm line increases upto 3 mole% and then decreases[ii].

CIE chromacity

The CIE Co-ordinates of dominant emission wavelength resulting in green light with chromaticity coordinates of (x = 0.251363409, y = 0.736605581) is shown in Fig. 9. For 543 nm the coordinates obtained fall at the border of Green region in the CIE 1931 chromaticity diagram and shown as black triangle shaped spot.

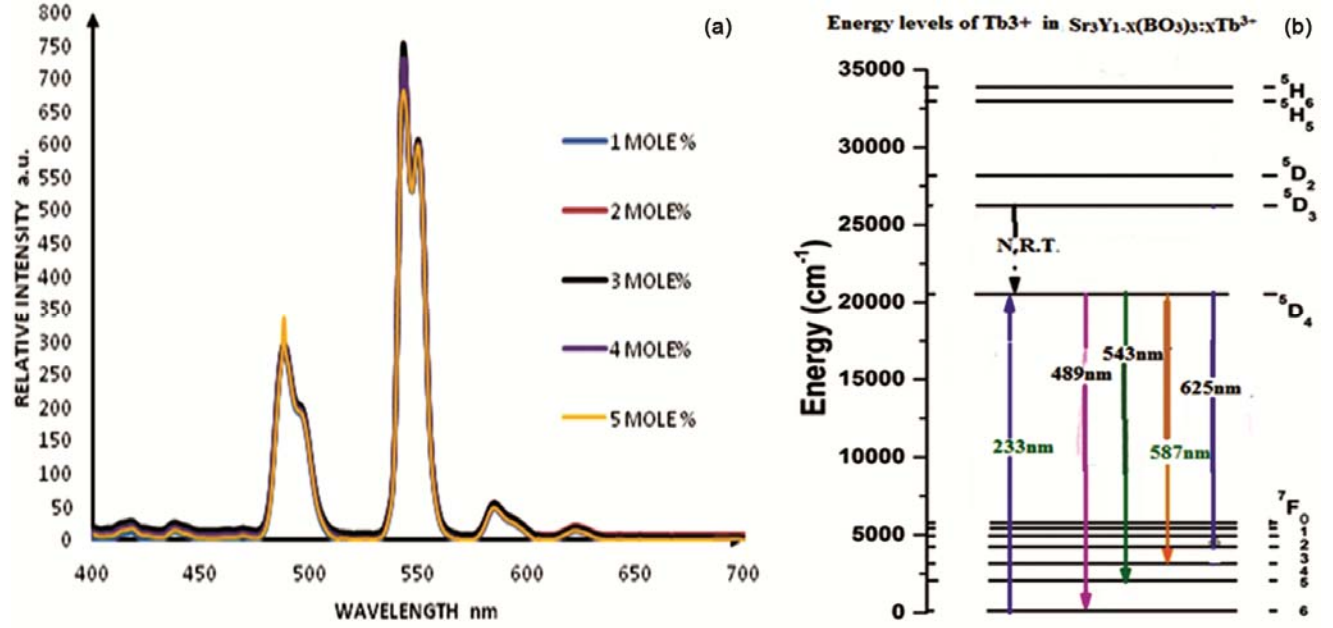

Fig. 7 — (a) PL properties for $^5D_4$ to $^7F_5$ transition of SYB with different doping concentrations of Tb^{3+} & (b) Energy levels of Tb^{3+} in SYB:Tb

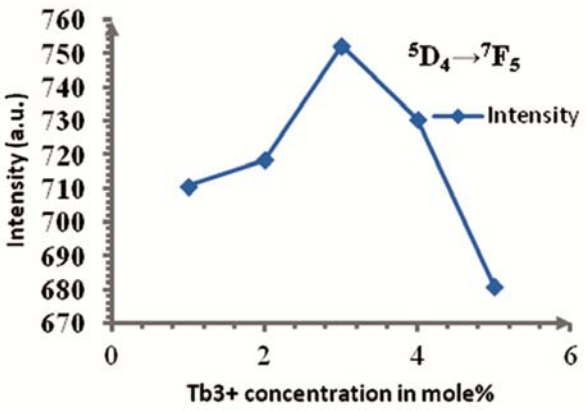

Fig. 8 — Concentration variation of Tb^{3+} ions in SYB phosphor

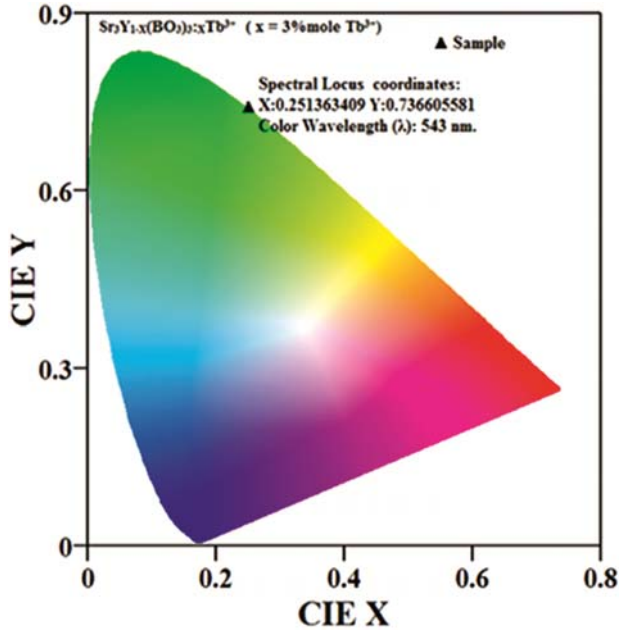

Fig. 9 — CIE diagram of $Sr_3Y_{1-0.03}(BO_3)_3{:}_{0.03}Tb^{3+}$ phosphor

Conclusions

In summary, SYB:Tb phosphors with the average size of about 0.5–2 μm were successfully deposited by a solution–combustion method, using rare-earth nitrates, urea and boric acid as starting materials. The crystal structure, morphology, chemical composition and photoluminescence properties of the films were investigated by X-ray diffraction (XRD) and scanning electron microscopy (SEM/EDS). Phosphors show three emission transitions of $^5D_4 \rightarrow {}^7F_J$ (J = 3, 4, 5) and among them, the transition $^5D_4 \rightarrow {}^7F_5$ displays the green (543 nm) color. The relationship between the luminescent intensity and the concentration of activated ions Tb^{3+} shows that there is concentration quenching of Tb^{3+} in host SYB and optimum concentration of Tb^{3+} in phosphor is 3 mol%. So the phosphor SYB:Tb may be predicted as a promising green phosphor candidate for applications in LED-based solid-state lighting or other display devices. The CIE of SYB:Tb was (x = 0.2513, y = 0.7366) with high color of green emission.

Acknowledgement

This work was supported by Physics Department, S.G.B.A.U. Amravati. We are Thankful to Head, Department of Physics S.G.B.A.U. for providing PLE-PL and XRD facility.

References

1 Xiao Y, Hao Z, Zhang L, Zhang X, Pan G H, Wu H, Luo Y & Zhang J, *J Mater Chem C*, 6 (2018) 5984.
2 Verma S, Verma K, Kumar D, Chaudhary B, Som S, Sharma V, Kumar V & Swart H C, *Phys B Condens Matter*, 535 (2017) 106.
3 Liu Y F, Silver J, Xie R J, Zhang J H, Xu H W, Shao H Z, Jiang J J & Jiang H C, *J Mater Chem C*, 5 (2017) 12365.
4 Liu Y F, Zhang J X, Zhang C H, Xu J T, Liu G Q, Jiang J J & Jiang H C, *Adv Opt Mater*, 3 (2015) 1096.
5 T Nishida, T Ban & N Kobayashi, *Appl Phys Lett*, 82 (2003) 3817.
6 Xie R J, Hirosaki N, Mitomo M, Sakuma K & Kiumra N, *Appl Phys Lett*, 89 (2006) 241103.
7 Daicho H, Iwasaki T, Enomoto K, Sasaki Y, Maeno Y, Shinomiya Y, Aoyagi S, Nishibori E, Sakata M, Sawa H, Matsuishi S & Hosono H, *Nat Commun*, 3 (2012) 1132.
8 Hirosaki N, Xie R, Inoue K, Sekiguchi T, Dierre B & Tamura K, *Appl Phys Lett*, 91 (2007) 061101 .
9 Geng D, Li G, Shang M, Peng C, Zhang Y, Cheng Z & Lin J, *Dalton Trans*, 41 (2012) 3078.
10 Wang X, Zhao Z, Wu Q, Li Y & Wang Y, *Inorg Chem*, 55 (2016) 11072.
11 Sun J, Ding D & Sun J, *Opt Mater*, 58 (2016) 188.
12 Lin Y C, Karlsson M & Bettinelli M, *Top Curr Chem*, (Z) 374 (2016) 309.
13 Haumesser P H, Gaume R, Benitez J M, Viana B, Ferrand B, Aka G & Vivien D, *J Cryst Growth*, 233 (2001) 233.
14 Denault K A, Cheng Z, Brgoch J, Den Baars S P & Seshadri R, *J Mater Chem C*, 1 (2013) 7339.
15 Simura R, Kawai S, Sugiyama K, Yanagida T, Sugawara T, Shishido T & Yoshikawa A, *J Cryst Growth*, 362 (2013) 296.
16 Palaspagar R S, Sonekar R P & Omanwar S K, *J Mater Sci Mater Electron*, 27 (2016) 4951.
17 Palaspagar R S, Gawande A B, Sonekar R P & Omanwar S K, *Mater Res Bulletin*, 72 (2015) 215.
18 Palaspagar R S, Gawande A B, Sonekar R P & Omanwar S K, *J Chin Chem Soc*, 3 (2015) 170.